Variability in Global Top-of-Atmosphere Shortwave Radiation Between 2000 and 2005

Norman G. Loeb[1], Bruce A. Wielicki
NASA Langley Research Center, Hampton University, Hampton, Virginia

Fred G. Rose, David R. Doelling
Analytical Services & Materials Inc., Hampton, Virginia

Geophysical Research Letters
Submitted September, 2006

[1] *Corresponding Author Address*: Dr. Norman G. Loeb, Mail Stop 420, NASA Langley Research Center, Hampton, VA 23681-2199, U.S.A. (757) 864-5688 (office); (757) 864-7996 (fax);

Email: n.g.loeb@larc.nasa.gov

Abstract

Measurements from various instruments and analysis techniques are used to directly compare changes in Earth-atmosphere shortwave (SW) top-of-atmosphere (TOA) radiation between 2000 and 2005. Included in the comparison are estimates of TOA reflectance variability from published ground-based Earthshine observations and from new satellite-based CERES, MODIS and ISCCP results. The ground-based Earthshine data show an order-of-magnitude more variability in annual mean SW TOA flux than either CERES or ISCCP, while ISCCP and CERES SW TOA flux variability is consistent to 40%. Most of the variability in CERES TOA flux is shown to be dominated by variations global cloud fraction, as observed using coincident CERES and MODIS data. Idealized Earthshine simulations of TOA SW radiation variability for a lunar-based observer show far less variability than the ground-based Earthshine observations, but are still a factor of 4-5 times more variable than global CERES SW TOA flux results. Furthermore, while CERES global albedos exhibit a well-defined seasonal cycle each year, the seasonal cycle in the lunar Earthshine reflectance simulations is highly variable and out-of-phase from one year to the next. Radiative transfer model (RTM) approaches that use imager cloud and aerosol retrievals reproduce most of the change in SW TOA radiation observed in broadband CERES data. However, assumptions used to represent the spectral properties of the atmosphere, clouds, aerosols and surface in the RTM calculations can introduce significant uncertainties in annual mean changes in regional and global SW TOA flux.

1. Introduction

The amount of solar radiation absorbed by the Earth is the principle source of energy that drives the climate system. It is determined from the difference between how much solar radiation is intercepted by the planet and how much is reflected back to space. Over a year, a planetary radiation balance is approached whereby the absorbed solar radiation is nearly balanced by outgoing terrestrial infrared radiation. A change in planetary albedo could significantly modify this balance and alter climate. For example, an increase in albedo would mean less solar heating and offset the influence of increased absorption of infrared radiation in the atmosphere due to the buildup of CO2, CH4, and other greenhouse gases. Sensitivity studies show that an absolute increase (decrease) in planetary albedo of 0.01 could potentially lead to a decrease (increase) in equilibrium surface temperature by as much as 1.75°C (Cess, 1976).

Recently a number of publications have emerged showing contradictory changes in planetary albedo during the first part of the 21st century. Using ground-based measurements of Earthshine, Pallé et al. (2004) find that the Earth's reflectance has increased by as much as 0.018 between 1999 and 2003, corresponding to a change of ~6 Wm^{-2} in top-of-atmosphere (TOA) radiative flux ($\Delta F = \Delta\alpha \times C/4$, where F=TOA flux, α=albedo, C=1365 Wm^{-2}). Pallé et al. (2004) estimate the Earth's albedo using telescope measurements of the visible solar radiation that is first reflected by the Earth towards the Moon and then back from the Moon to an observer on the night-side of the Earth at the Big Bear Solar Observatory (BBSO) in California. The ground-based Earthshine measurements (Pallé et al., 2004) sample only ~1/3 of the Earth on any given day, and cover at most ~1/3 of each lunar month provided the night-sky is cloud-free. A 6 Wm^{-2}

change is climatologically significant as it exceeds the radiative forcing caused by Mount Pinatubo in the early 1990s by a factor of 2.5, and is twice as large as the longwave radiative forcing by greenhouse gases since 1850 (Houghton et al., 2001). Pallé et al. (2004) find support for this result from variations in the satellite on-board temperatures of the Global Ozone Monitoring Experiment (GOME) instrument, which are hypothesized to be influenced by changes in Earth's outgoing radiance (Casadio et al., 2005). In contrast, the global CERES observations show a small decrease of ~2 Wm^{-2} in shortwave reflected flux between 2000 and 2004 (Wielicki et al., 2005). More recently, Loeb et al. (2006) used a revised version of the CERES data to show that no statistically significant changes in the Earth's albedo have occurred between 2000 and 2005. Their results are consistent with changes in Photosynthetically Active Radiation (PAR) during the same period from Sea-Viewing Wide-Field-of-View Sensor (SeaWiFS) TOA radiance measurements (Patt et al., 2003) for all-sky conditions over ocean. PAR is defined as the solar flux reaching the ocean surface in the 400-700 nm spectral range and is anti-correlated to SW TOA flux. Loeb et al. (2006) also found consistent results between CERES monthly SW TOA flux anomalies and those from the International Satellite Cloud Climatology Project (ISCCP) radiative flux profile data set (ISCCP-FD product) (Zhang et al., 2004).

In this study, several different approaches for monitoring the variability in the Earth's TOA SW Radiation are considered. In Section 2 we perform simulations of lunar-based Earthshine measurements in order to assess whether or not this approach is suitable for monitoring changes in the Earth's albedo. In Section 3 we compare temporal changes in TOA SW radiation using radiative transfer models initialized with retrievals from the

Moderate Resolution Imaging Spectroradiometer (MODIS) with coincident radiative fluxes obtained directly from CERES broadband measurements. Finally, Section 4 compares annual anomalies in SW TOA flux from ground-based Earthshine, CERES and ISCCP between 2000 and 2005, as well as monthly anomalies from CERES SW TOA flux and MODIS cloud fraction.

2. Seasonal Cycle of Albedo

Global albedo has a distinct and repeatable seasonal cycle. Because of the tilt of the Earth's axis and the large surface albedo of snow at high latitudes, it reaches maximum values during the solstice months and minimum values during the equinox months. Changes in cloud and surface properties from year to year introduce slight variations in the seasonal cycle of albedo, but these perturbations are much smaller than the basic seasonal cycle of albedo. As a minimum, therefore, any approach that attempts to measure subtle changes in the Earth's albedo must be able to characterize the broad features of global albedo changes with season.

Here we simulate the seasonal cycle of the Earth's reflectance as it would appear from an observer on the moon viewing Earthshine. The simulation uses CERES Angular Distribution Models (ADMs) (Loeb et al., 2003) and measurements from CERES Terra Single Satellite Footprint (SSF) product for 2002 through 2004. Assuming no changes in scene properties between the CERES and Earthshine measurement times, we can simulate the reflectance contributions from all points on the Earth that contribute to Earthshine by using the CERES ADMs to transform the observed reflectance at the CERES viewing geometry to that corresponding to the sun-earth-moon viewing geometry at the Earthshine observation time. These reflectances are then integrated over the lunar

viewing geometry to determine the total Earthshine reflectance intercepted by the moon. Conceptually, we can think of the moon as a satellite measuring the Earth's reflectance over a large portion of the Earth from a viewing geometry defined by the relative position of the sun, earth and moon. To calculate the sun-earth-moon geometry, the Science Data Production Toolkit for the Earth Observing System Data and Information System (EOSDIS) Core System (ECS) is used. For each day, the Earthshine simulation is updated hourly. Following Pallé et al. (2004), only observations with a lunar phase angle between 65° and 135° are considered. To remove reflectance variations due to changes in lunar viewing geometry during the lunar month, the reflectance at every time-step is adjusted to a common lunar phase angle of 95° using a 5^{th}-order polynomial regression fit of Earthshine reflectance against lunar phase angle for data between 2002 and 2004. Because the lunar observer is assumed to collect data continuously throughout the day from all parts of the Earth that contribute to Earthshine, the spatial and temporal sampling in this simulation is more complete than the ground-based Earthshine measurements of Pallé et al. (2004), which are restricted to a few hours per night and limited to cloud-free conditions at one site (BBSO). The lunar Earthshine simulation represents ideal sampling conditions: it is analogous to having multiple ground-based Earthshine sites around the globe with no intercalibration differences, no cloud coverage restrictions, and since CERES SW data are considered, no narrow-to-broadband conversion errors.

Because of Terra's sun-synchronous 98° inclination orbit and the wide swath width of CERES, CERES acquires global coverage on a daily basis. The first step to determining global albedo from CERES Terra radiance measurements is to apply CERES ADMs to convert measured radiances to radiative flux values (Loeb et al., 2005). Each

instantaneous TOA flux is converted to a 24-hour TOA flux by applying diurnal albedo models that account for albedo changes at all times of the day, assuming the scene at the CERES *Terra* overpass time remains invariant throughout the day. This assumption is found to have a negligible effect on the interannual variability of albedo at global scales. The diurnal albedo models were derived from ADMs developed from CERES measurements on the Tropical Rainfall Measuring Mission Satellite (TRMM) (Loeb et al., 2003). TOA fluxes from each day are then placed on a 1°×1° latitude-longitude equal-area nested grid and averaged over the month. A global monthly mean albedo is determined from the ratio of the global monthly mean SW TOA flux to the global mean solar insolation at the TOA for the month.

Fig. 1a-b compares the seasonal cycle in simulated Earthshine reflectance and CERES global albedo given as the deviation from the mean 3-year value for 2002 through 2004. CERES global albedos exhibit a well-defined seasonal cycle with albedo maxima and minima occurring at the same time of year for each of the 3 years. In contrast, while a seasonal cycle in Earthshine reflectance is apparent in Fig. 1a, it is highly variable and out-of-phase from one year to the next. As a result, the year-to-year variability in a given month is typically 4-5 times larger for Earthshine reflectance compared to CERES albedo.

3. Temporal Variations in TOA SW Radiation Using Radiative Transfer Models

An alternate way of inferring broadband TOA albedo is through radiative transfer model (RTM) calculations with input cloud, atmosphere and surface properties derived from global measurements. This approach is used in the International Satellite Cloud Climatology Project (ISCCP) (Rossow et al., 1999) to create the ISCCP-FD data product

which contains global 280-km radiative fluxes at 3-hour time steps (Zhang et al., 2004). The CERES project also provides radiative fluxes that are based on RTM calculations with cloud and aerosol properties from MODIS measurements (Wielicki et al., 1996; Charlock et al., 1997). This dataset, called the Clouds and Radiative Swath (CRS) data product, provides TOA fluxes at the CERES footprint scale at the CERES time of observation. Calculated radiative fluxes in the CRS product are independent of those in the CERES SSF data product, which are inferred directly from CERES broadband radiance measurements (Loeb et al., 2005). Since narrowband radiance measurements are the primary inputs, the RTM approach involves an approximation of the spectral and bidirectional properties of the atmosphere, clouds, aerosols and the surface over the globe. In order to assess the suitability of the RTM approach to characterize temporal variations in SW radiation, we compare the change in regional annual mean SW TOA flux distribution between 2004 and 2001 based on the RTM approach with that based on radiative fluxes from CERES SSF product using the following expression:

$$\Delta F_{04-01}(\lambda,\phi) = \Delta F^{CRS}_{04-01}(\lambda,\phi) - \Delta F^{SSF}_{04-01}(\lambda,\phi) \quad (1)$$

where ΔF^{CRS}_{04-01} represents the difference in annual mean SW TOA flux between 2004 and 2001 in the CRS data product, ΔF^{SSF}_{04-01} is the corresponding difference from the SSF data product, and (λ,ϕ) corresponds to the latitude-longitude region. ΔF_{04-01} is converted to an equivalent 24-h average daily mean value by applying scaling factors derived from the CERES Monthly TOA/Surface Averages (SRBAVG) and SSF data products. Results in Fig. 2 show that the RTM approach underestimates the SW TOA flux change between 2004 and 2001 over land by up to 8 Wm^{-2} (e.g., over central Asia), and overestimates the flux change over the desert. Over ocean, the errors are smaller, but they exhibit a slight

dependence upon latitude. Fig. 3 shows deseasonalized anomalies in the relative difference between CRS and SSF reflected SW TOA flux for global ocean and land. Anomalies in the relative difference generally remain within ±1.5%, and differ between ocean and land by up to 1% in 2001. While fluctuations in CRS-SSF relative difference anomalies with time are undoubtedly partly due to relative calibration changes between CERES and MODIS (Loeb et al., 2006), the differences between ocean and land suggest that narrow-to-broadband errors in the RTM approach (e.g., due to the assumed spectral properties of the atmosphere, clouds, aerosols and surface) are also significant and can introduce appreciable uncertainties in SW TOA flux changes.

4. SW TOA Flux Anomalies

An overall summary of annual anomalies in SW TOA flux between 2000 and 2004 based on several different methods is provided in Fig. 4a. The Earthshine BBSO results are from Pallé et al. (2004), while "CERES global" results are based on global SW TOA fluxes from the SSF data product that have been converted to 24-h average fluxes by applying diurnal albedo models that account for albedo changes at all times of the day, assuming the scene at the CERES *Terra* overpass time remains invariant throughout the day (Loeb et al., 2006). ISCCP-FD global albedo anomalies are from Zhang et al. (2004), while the "CERES Earthshine Simulation" results correspond to simulations described in Section 2. Anomalies based on CERES CRS TOA fluxes are not included because diurnal average fluxes based on instantaneous CRS TOA fluxes were unavailable at the time of this study. The most striking feature in Fig. 4a is the marked difference between Earthshine (BBSO) (Pallé et al., 2004) anomalies and all other methods. None of the other methods support the dramatic increase in BBSO Earthshine reflectance between

2000 and 2003. The standard deviation in the BBSO Earthshine anomalies is a factor of 5 greater than the simulated CERES Earthshine anomalies, and over an order-of-magnitude greater than those from CERES global results. Interestingly, anomalies based on the simulated CERES Earthshine approach bear little resemblance to the CERES global results. In fact, the standard deviation in the simulated CERES Earthshine anomalies is a factor of 2 larger than the CERES global results. While ISCCP and CERES SW TOA flux anomalies also differ from one another from year to year, the standard deviation in the anomalies is within 40% of each other.

Although anomalies based on CERES CRS TOA fluxes are not yet available for comparison, it is possible to compare monthly anomalies in global mean CERES SW TOA flux and MODIS cloud fraction, as shown in Fig. 4b. The strong correlation between the anomalies in these two variables implies that most of the monthly variation in SW TOA flux is associated with changes in cloud cover. The remaining variability is likely associated with cloud optical depth variations and to a lesser extent surface albedo variations.

5. Conclusions

Monitoring changes in the Earth's SW TOA radiation is critical for understanding climate. However, because of the spatial and temporal scales involved and the need to account for radiant energy across the entire solar spectrum, it presents a significant observational challenge: all methods that attempt to measure the Earth's TOA radiation suffer from sampling errors due to inadequate spatial, temporal or spectral coverage. This study considers results from three independent approaches and compares recent changes in TOA SW radiation between 2000 and 2005. The Earthshine ground-based approach of

Pallé et al. (2004) shows the largest variability in annual mean SW TOA radiation, reaching 6 Wm^{-2} between 1999 and 2003. Simulations of lunar Earthshine measurements show far less variability than those observed from the ground by Pallé et al. (2004), but still show 4-5 times the variability observed from CERES global data. Furthermore, while CERES global albedos exhibit a well-defined seasonal cycle with albedo maxima and minima occurring at the same time each year, the seasonal cycle in lunar Earthshine reflectance simulations is highly variable and out-of-phase from one year to the next. Radiative transfer model (RTM) approaches that use imager cloud and aerosol retrievals reproduce most of the change in SW TOA radiation observed in broadband CERES data, but the assumptions used to represent the spectral properties of the atmosphere, clouds, aerosols and surface in the RTM calculations can introduce significant uncertainties in annual mean changes in regional and global SW TOA flux. Such uncertainties can cause interannual anomaly errors ranging from 1% for global ocean to 2% for global land, much too large for climate change decadal signals.

The largest uncertainty in global climate sensitivity over the next century is cloud feedback. Since global cloud feedback has been shown to be linear in changing cloud radiative forcing (CRF) (Soden and Held, 2006), this implies that changes in net CRF are directly related to climate sensitivity. The difficulty in documenting climate variability and change is in the calibration stability requirements. Estimates of anthropogenic total radiative forcing in the next few decades are 0.6 Wm^{-2} per decade (Houghton et al., 2001). A 25% cloud feedback would change cloud net radiative forcing by 25% of the anthropogenic radiative forcing, or 0.15 Wm^{-2} per decade. The global average shortwave (SW) or solar reflected cloud radiative forcing by clouds is ~50 Wm^{-2}, so that the

observation requirements for global broadband radiation budget to directly observe such a cloud feedback is approximately 0.15/50 = 0.3% per decade in SW broadband calibration stability (Ohring et al., 2005). Achieving this stability per decade in calibration is extremely difficult and has only recently been demonstrated for the first time by the ERBS and CERES broadband radiation budget instruments (Wong et al., 2006; Loeb et al., 2006).

Acknowledgements

The CERES data are provided by the NASA Langley Atmospheric Sciences Data Center in Hampton, Virginia. The ISCCP FD data set is obtained directly on-line from the ISCCP web site at isccp.giss.nasa.gov. The NASA Science Mission Directorate through the CERES project at Langley Research Center funded this study.

References

Casadio, S., A. di Sarra, and G. Pisacane, 2005: Satellite on-board temperatures: Proxy measurements of Earth's climate changes?, *Geophys. Res. Lett.*, **32**, L06704, doi:10.1029/2004GL022138.

Cess, R.D., 1976: Climate change: An appraisal of atmospheric feedback mechanisms employing zonal climatology, *J. Atmos. Sci*., **33**, 1831-1843.

Charlock, T. P., F. G. Rose, D. A. Rutan, T. L. Alberta, D. P. Kratz, L.H. Coleman, G. L. Smith, N. Manalo-Smith, and T. D. Bess, 1997: Compute Surface and Atmospheric Fluxes (System 5.0), CERES Algorithm Theoretical Basis Document. 84 pp., [Available from http://asd-www.larc.nasa.gov/ATBD/pdf_docs/r2_2/ceres-atbd2.2-s5.0.pdf].

Houghton et al., 2001: Intergovernmental Panel on Climate Change (IPCC), Climate Change 2001: The Scientific Basis. Contribution of Working Group I to the Third Assessment Report of the Intergovernmental Panel on Climate Change (IPCC), J. T. Houghton et al., Eds. (Cambridge Univ. Press, Cambridge, 2001).

Loeb, N. G., N. M. Smith, S. Kato, W. F. Miller, S. K. Gupta, P. Minnis, and B. A. Wielicki, 2003: Angular distribution models for top-of-atmosphere radiative flux estimation from the Clouds and the Earth's Radiant Energy System instrument on the Tropical Rainfall Measuring Mission Satellite. Part I: Methodology, *J. Appl. Meteor*., 42, 240-265.

Loeb, N. G., S. Kato, K. Loukachine, and N. M. Smith, 2005: Angular distribution models for top-of-atmosphere radiative flux estimation from the Clouds and the

Earth's Radiant Energy System instrument on the *Terra* Satellite. Part I: Methodology, *J. Ocean and Atmos. Tech.*, 22, 338-351.

Loeb, N.G., B.A. Wielicki, W. Su, K. Loukachine, W. Sun, T. Wong, K.J. Priestley, G. Matthews, W.F. Miller, and R. Davies, 2006: Multi-Instrument Comparison of Top of the Atmosphere Reflected Solar Radiation, *J. Climate* (in press).

Ohring, G., B. A. Wielicki, R. Spencer, B. Emery, and R. Datla, 2005: Satellite instrument calibration for measuring global climate change: Report of a Workshop, *Bull. Amer. Met. Soc*., **86**, 1303-1313.

Pallé, E., P. R. Goode, P. Montañés-Rodriguez, and S. E. Koonin, 2004: Changes in the Earth's reflectance over the past two decades, *Science*, **304**, 1299–1301, doi:10.1126/science.1094070.

Patt, F. S., R. A. Barnes, R. E. Eplee, Jr., B. A. Franz, W. D. Robinson, G. C. Feldman, S. W. Bailey, J. Gales, P. J. Werdell, M. Wang, R. Frouin, R. P. Stumpf, R. A. Arnone, R. W. Gould, Jr., P. M. Martinolich, V. Ransibrahmanakul, J. E. O'Reilly, and J. A. Yoder, 2003: Algorithm updates for the fourth SeaWiFS data reprocessing, NASA Tech. Memo. 2003--206892, 22, S.B. Hooker and E.R. Firestone, Eds., NASA Goddard Space Flight Center, Greenbelt, Maryland, 74 pp. [Available online from: http://oceancolor.gsfc.nasa.gov/cgi/postlaunch_tech_memo.pl?22]

Rossow, W. B., and R. A. Schiffer (1999), Advances in understanding clouds from ISCCP, *Bull. Am. Meteorol. Soc*., **80**, 2261– 2287.

Soden, B.J., and I.M. Held, 2006: An assessment of Climate Feedbacks in Coupled Ocean–Atmosphere Models, *J. Climate*, **19**, 3354-3360.

Wielicki, B. A., B. R. Barkstrom, E. F. Harrison, R. B. Lee, G. L. Smith, and J. E. Cooper, 1996: Clouds and the Earth's Radiant Energy System (CERES): An Earth Observing System Experiment. *Bull. Amer. Meteor. Soc*., **77**, 853-868.

Wielicki, B.A., T. Wong, N.G. Loeb, P. Minnis, K.J. Priestley, R. Kandel, 2005: Changes in Earth's albedo measured by satellite, *Science*, **308**, p. 825.

Wong, T., B. A. Wielicki, R. B. Lee, III, G. L. Smith, and K. A. Bush, 2006: Re-examination of the observed decadal variability of Earth radiation budget using altitude-corrected ERBE/ERBS Nonscanner WFOV data, *J. Climate* (in press).

Zhang, Y., W. B. Rossow, A. A. Lacis, V. Oinas, and M. I. Mishchenko (2004), Calculation of radiative fluxes from the surface to top of atmosphere based on ISCCP and other global data sets: Refinements of the radiative transfer model and the input data, *J. Geophys. Res*., **109**, D19105, doi:10.1029/2003JD004457.

Figures

Figure 1 Seasonal variation in (a) simulated Earthshine reflectance and (b) CERES global albedo expressed as the deviation from the 3-year mean value. Earthshine reflectances are adjusted to a common lunar phase angle of 95°.

Figure 2 Change in regional annual mean SW TOA flux distribution between 2004 and 2001 based on the RTM approach with that based on radiative fluxes from CERES SSF product.

Figure 3 Deseasonalized anomalies in the relative difference between CRS and SSF reflected SW TOA flux for global ocean and land from CERES and MODIS Terra observations.

Figure 4 (a) Global annual mean SW TOA flux anomalies from Earthshine BBSO (Palle et al., 2005), CERES Terra global fluxes, ISCCP-FD, and a simulation of Earthshine. (b) Monthly anomalies in global mean CERES SW TOA flux and MODIS cloud fraction.

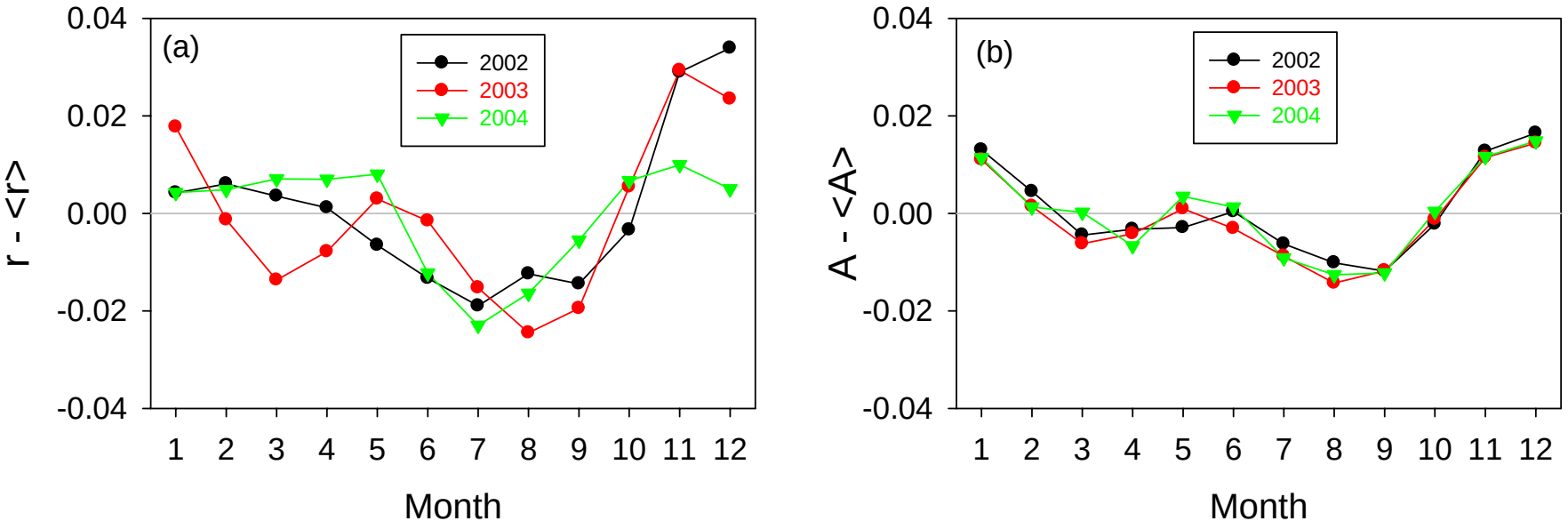

Figure 1 Seasonal variation in (a) simulated Earthshine reflectance and (b) CERES global albedo expressed as the deviation from the 3-year mean value. Earthshine reflectances are adjusted to a common lunar phase angle of 95°.

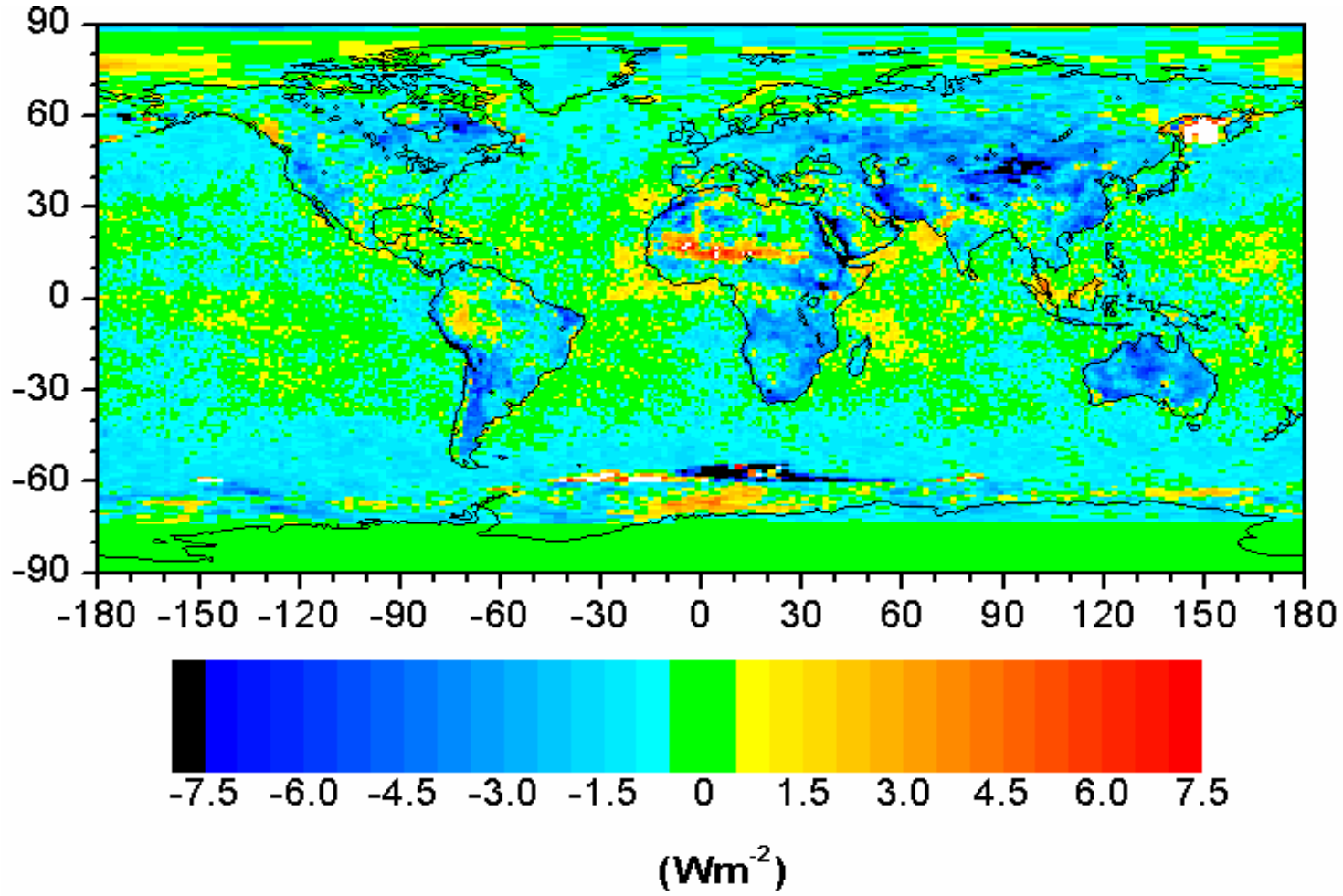

Figure 2 Change in regional annual mean SW TOA flux distribution between 2004 and 2001 based on the RTM approach with that based on radiative fluxes from CERES SSF product.

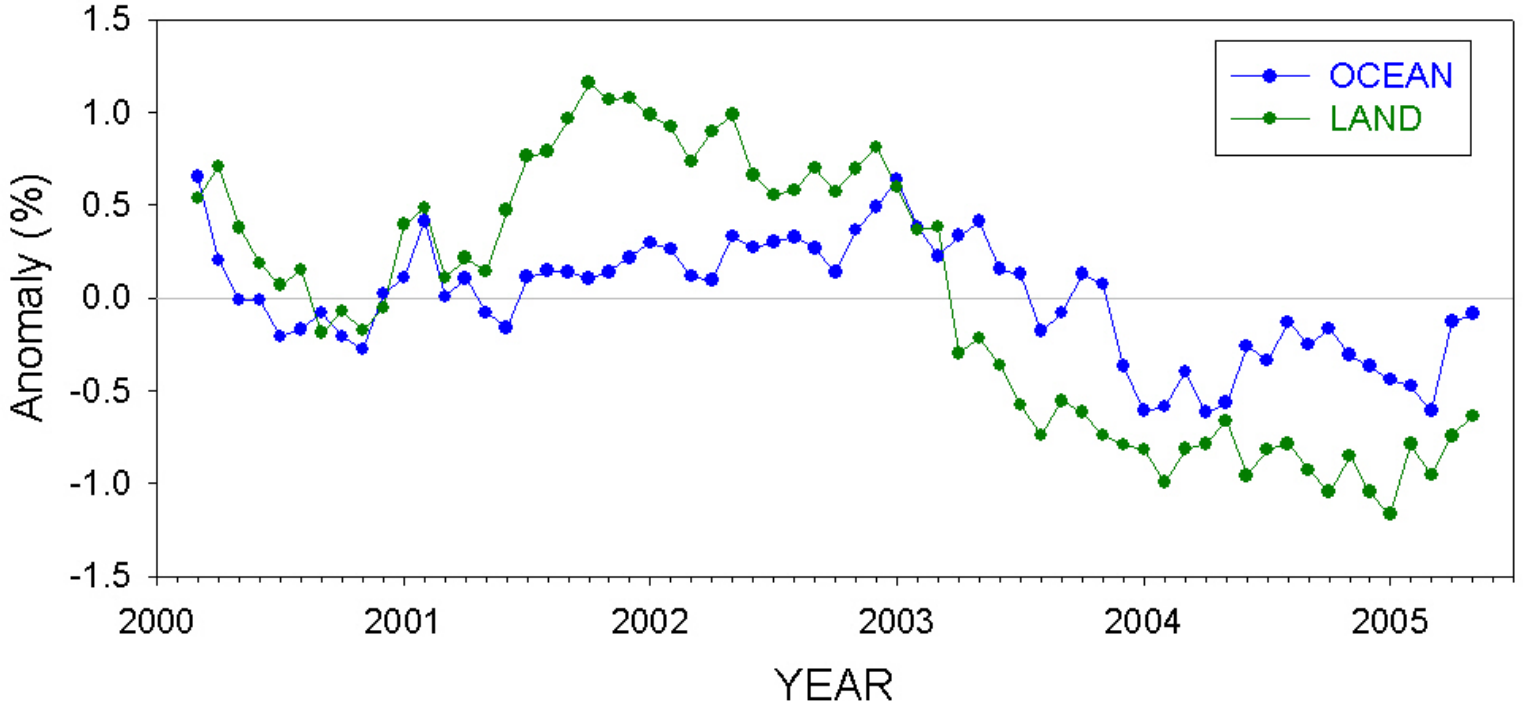

Figure 3 Deseasonalized anomalies in the relative difference between CRS and SSF reflected SW TOA flux for global ocean and land from CERES and MODIS Terra observations.

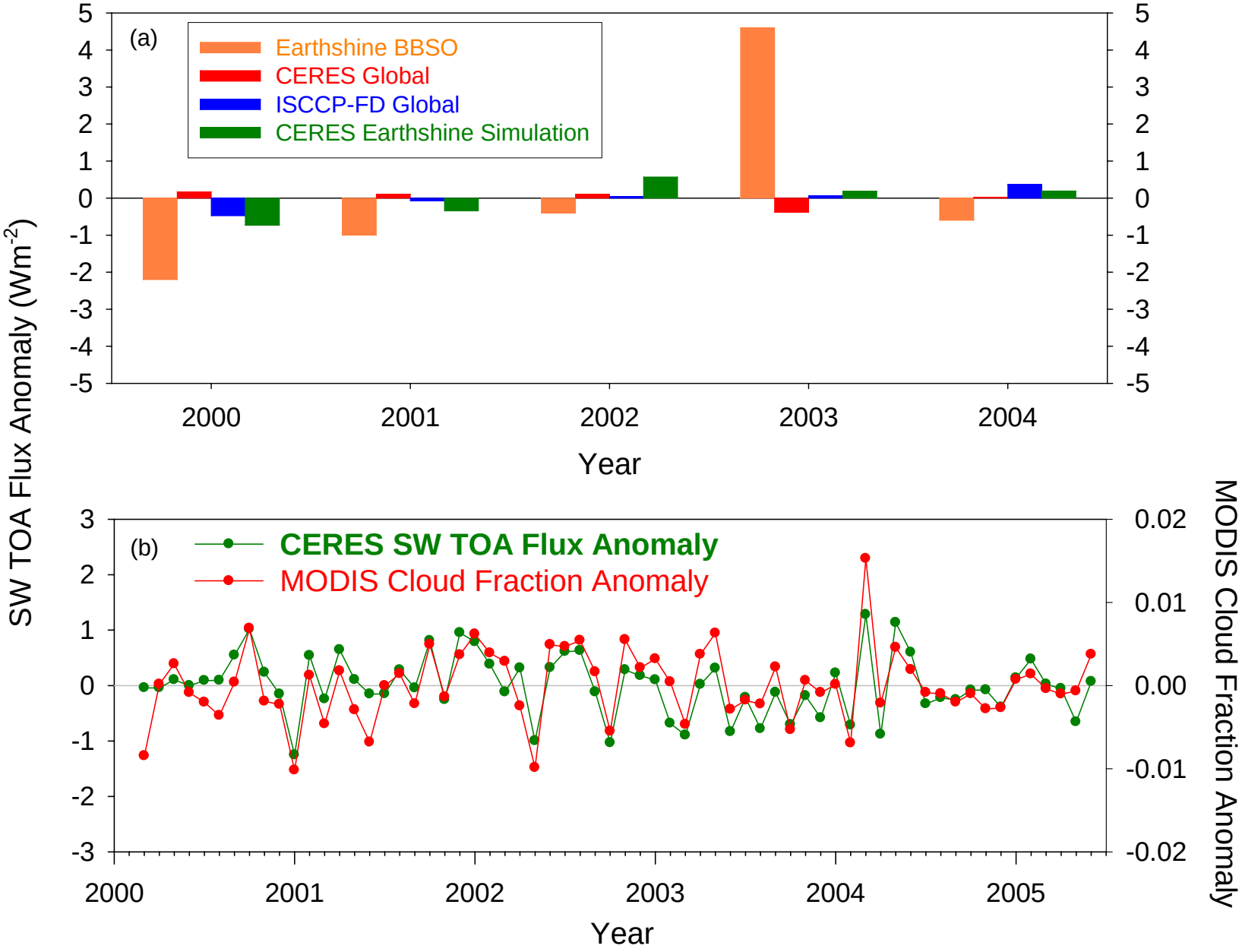

Figure 4 (a) Global annual mean SW TOA flux anomalies from Earthshine BBSO (Palle et al., 2005), CERES Terra global fluxes, ISCCP-FD, and a simulation of Earthshine. (b) Monthly anomalies in global mean CERES SW TOA flux and MODIS cloud fraction.